PERGAMON

Control Engineering Practice 7 (1999) 383–390

6 DOF dynamic localization of an outdoor mobile robot

Ph. Bonnifait*, G. Garcia

Institut de Recherche en Cybernétique de Nantes, U.M.R. 6597 Ecole Centrale de Nantes 1, rue de la Noë, BP 92101, 44321 Nantes Cedex 3, France

Received 23 March 1998; accepted 30 September 1998

Abstract

A novel design of a three-dimensional localizer intended for outdoor mobile robots is presented. By integrating data from two inclinometers and an odometer, the system provides high-frequency position and attitude data. The unavoidable dead-reckoning location divergence is corrected by using the azimuth and elevation angles of known landmarks, provided by a rotating linear camera. Even if these measurements are intermittent and are obtained at a low frequency and one at a time, simulations indicate that the formalism proposed in this paper is able to reach an accuracy of a few centimeters on the elevation. Finally, real experiments performed with an outdoor mobile robot are presented and analyzed.

Keywords: Mobile robots; Navigation systems; Position and attitude estimation; Multisensor integration; Kalman filters

1. Introduction

This paper presents a localization system which is intended for later use in the context of computer-integrated road construction (CIRC). However, the principle of the method is of general relevance to robotics.

The peculiarity of civil-engineering tasks is that some of them require the six degrees of freedom (DOF) of the machine or of its tool to be determined, with high precision. For example, the finishing process (applying the final layer of the road) requires a 0.1° precision on the roll and pitch angles. For this same task, a 1 cm precision or better is desired on the altitude. These are very tight precision levels. On the other hand, the machines to which the system should be applied are very slow, typically 0.1 m/s in the highest-precision task of the road finishing process (Le Corre and Garcia, 1992). In such a context, dynamics and accelerations are very small and, thus, the use of inclinometers is attractive since they directly provide attitude angles. Here, their comparatively slow response does not degrade the estimation process. In contrast, dead reckoning based on strap-down-type inertial units is suited to more dynamic applications. Several variants of solutions based on accelerometers and/or gyros can be found in the literature. For instance, six accelerometers alone (Chen et al., 1994) or redundant gyros (Rintanen et al., 1994) allow the computation of the angular and linear speeds. Mixed solutions can take advantage of both systems (Barshan and Durrant-Whyte, 1995; Vaganay et al., 1993).

Nevertheless, whatever the algorithmic solution, an absolute position sensor is necessary to overcome long-term drift, and to increase the reliability of the system. Moreover, the integration of dead-reckoning data does not allow a precise estimation of the elevation, which is a crucial parameter in the application of interest here. For these reasons, the inertial location is corrected using the azimuth and elevation angles of known beacons, the positions of which are accurately measured by surveyors. The Kalman filter formulation detailed in the following allows each goniometric measurement to be taken into account individually and asynchronously.

The paper is organized as follows. The sensors are described in Section 2. Section 3 is devoted to the 6 DOF position and attitude representation. A new attitude representation is proposed, which directly uses the parameters measured by the inclinometers. In Section 4, new 3D odometric equations are derived with two inclinometers, for a mobile moving on a non-planar

*Correspondence address: Univ. de. Technologie de Compiegne, Centre de Recherche de Royallieu, UMR CNRS 6599, Heuristique et Diagnostic des Systemes Complexes 60205 Compiegene cedex, France. Tel.: + 33 3 44 33 44 23; fax: + 33 3 44 23 44 77; e-mail: gaetan.garcia@ircyn.prd.fr.

0967-0661/99/$ – see front matter
PII: S0967-0661(98)00159-2

surface. Then, the Kalman filter formulation is described. In Section 5, the proposed method is evaluated through simulations. Finally, real experimental results are reported and analyzed in Section 6.

2. Description of the sensors

Fig. 1 shows the experimental setup. The external sensor is a linear CCD camera which rotates at a constant speed (≈ 1 rad/s) around an axis fixed to the vehicle. Artificial beacons (battery-powered twin-light sources) are placed in the environment at known locations. So, with three beacons, the camera detects, on average, a landmark every 2 s. These beacons are automatically switched on using a radio link, just before the rotary sensor is going to detect them. Once the reading has been taken, the light is switched off in order to decrease energy consumption. Hence, the landmarks are detected one at a time and intermittently. The maximum range of the system (i.e. the distance between a beacon and the sensor) is 40 m.

The azimuth angles (denoted λ) are measured with respect to the heading by an optical encoder. Simultaneously, the sensor measures the elevation angle (σ) between the camera's optic axis and the line that passes through the optical center and the beacon (cf. Fig. 1). Several existing systems rely on azimuth and elevation angles. For instance, in Tsumura et al. (1993), the localizer is made up of two laser scanners. Each one rotates a fan-shaped laser beam for detecting corner cubes, and measures azimuth and elevation angles. The system of Horn and Schmidt (1995) provides the same angles plus the distance between the sensor and the beacon, by using a camera and a 3D laser.

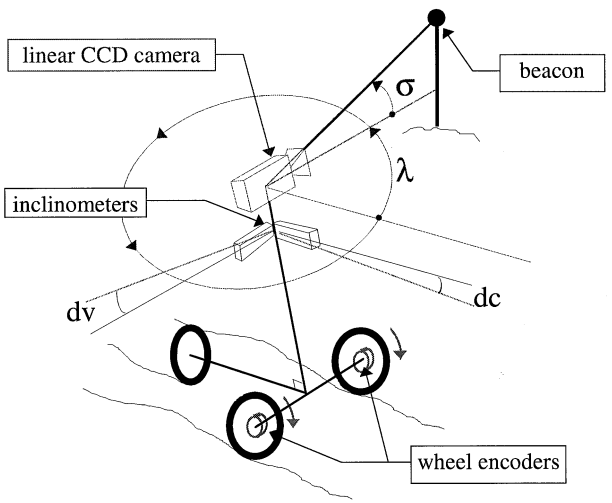

Fig. 1. The robot and its sensors.

The goniometric sensor has already been used successfully in 2D applications (Bonnifait and Garcia, 1996). Several tests performed in sunny weather conditions have proved the reliability of the system. It has also proved able to provide accurate 6 DOF data when used as a stand-alone sensor by deterministic algorithms, in static situations (Le Corre and Garcia, 1992). When the vehicle is moving, the measurements to the beacons do not correspond to the same positions. This problem can be solved by adding on-board sensors that allow a dead-reckoning localization to be computed. In other words, these additional sensors enable the movement of the vehicle between two external measurements to be estimated. Moreover, this approach improves the precision and robustness of the positioning system. For these reasons, the work described here uses two inclinometers and encoders mounted on two wheels of the robot (see Fig. 1). The pendulous inclinometers directly measure attitude angles of the mobile robot with respect to the gravity of the earth with a precision better than 0.1°, when the vehicle is motionless. The odometer provides the linear and angular speeds of the vehicle.

The multisensor integration presented in this paper is realized by an extended Kalman filter (EKF). This estimation method is very appropriate here because the noise, the redundancy and the complementarity of the sensors are naturally taken into account.

3. Choice of the state vector

In general, six independent variables are required to describe the posture (position and attitude) of a solid. Usually, position is given by the Cartesian coordinates, but as regards the attitude, many representations can be used. For instance, rotation matrices are given by roll-pitch-yaw angles (Fuke and Krotkov, 1996; Tsumura et al., 1993) or Euler angles (Barshan and Durrant-Whyte, 1995). These transformations have singularities but need only three parameters. On the other hand, quaternions (Rintanen et al., 1994; Vaganay et al., 1993) provide non-singular representations, but with four parameters.

A new attitude representation is presented here. This "geometrical" parameterization is defined by the direction angle ψ, the gradient dc and the orthogonal cross-fall dv (see Fig. 2) which are directly measured by the inclinometers. Eq. (1)–(6) give the attitude matrix as a function of ψ, dc and dv:

$$ {}^0\mathbf{A}_s = \begin{bmatrix} \cos(\psi)\cos(dc) & n_x & a_x \\ \sin(\psi)\cos(dc) & n_y & a_y \\ \sin(dc) & -\sin(dv) & \chi \end{bmatrix} \quad (1) $$

where

$$ \chi = \sqrt{\cos(dc)^2 - \sin(dv)^2} \quad (2) $$

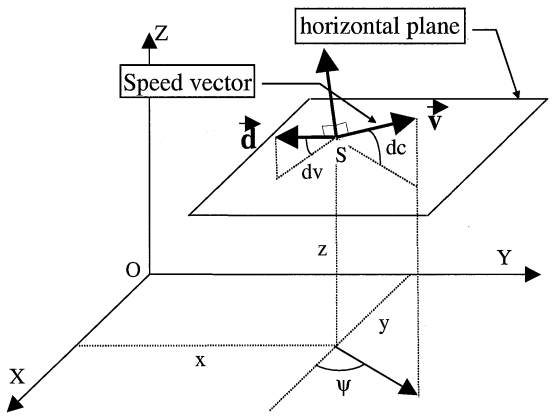

Fig. 2. Choice of the six independent parameters.

One can notice that the gradient and the cross-fall are not defined for $\pm \pi/2$. These situations never occur in realistic situations. Moreover, since $|dc| + |dc| < \pi/2$, χ is always defined.

$$n_x = -\frac{\sin(\psi)\chi - \cos(\psi)\sin(dc)\sin(dv)}{\cos(dc)} \quad (3)$$

$$n_y = \frac{\cos(\psi)\chi + \sin(\psi)\sin(dc)\sin(dv)}{\cos(dc)} \quad (4)$$

$$a_x = -\frac{\sin(\psi)\sin(dv) + \cos(\psi)\sin(dc)\chi}{\cos(dc)} \quad (5)$$

$$a_y = -\frac{-\cos(\psi)\sin(dv) + \sin(\psi)\sin(dc)\chi}{\cos(dc)} \quad (6)$$

The relations between (ψ, dc, dv) and the 'yaw-pitch-roll' angles (in this order) are given by:

$$\psi = yaw$$

$$dc = -pitch$$

$$\sin(dv) = -\sin(roll)\cdot\cos(pitch) \quad (7)$$

As the Cartesian position is used, the state vector to be estimated is:

$$X = [x \quad y \quad z \quad \psi \quad dc \quad dv]^T \quad (8)$$

4. Recursive 6 DOF estimation

The recursive state estimator is based on an EKF formulation. The odometric measured speeds are seen as the control input to the mobile and, therefore, appear in the *prediction phase* (20 Hz). As presented in a 2D case (Bonnifait and Garcia, 1996), the prediction error is computed using a linearized method. A *synchronized estimation phase* is performed with the inclinometer data, whereas a second *intermittent correction phase* (≈ 0.5 Hz) is done using the azimuth and elevation angles of a beacon. On average, this correction phase occurs every 40 prediction-estimation phases.

4.1. Odometry on a non-planar surface with two inclinometers

When moving on a non-planar surface, the posture of a mobile changes in three dimensions.

If the equation of the surface is known, Kim et al. (1996) describe a dead-reckoning method for a two-wheeled robot with two encoders. Except in particular applications, curved surfaces are unknown and this technique is not applicable. Fuke and Krotkov (1996) use encoders to calculate the velocity. By an EKF, they combine three gyros and three accelerometer signals and determine the attitude. Then, they incrementally update the position.

The approach presented below uses only four sensors: two encoders and two tilt sensors.

4.1.1. Principle

Let R_S be the robot frame to be localized. Suppose $\mathbf{X}_i$, the state vector at time i, is known. The goal is to compute $\mathbf{X}_{i+1}$, knowing $\mathbf{U}_i = [\Delta_i, \omega_i]^T$, the elementary translation and rotation measured by the odometer between times i and $i+1$, and (α_i, β_i) the measurements of the two inclinometers at time i.

Consider an auxiliary frame, denoted R_π, such that $(R_s)_i = (R_\pi)_i$. At time i, the origin Ω of R_π is equal to point S, the origin of R_s. While the robot moves between time indexes i and $i+1$, the frame R_π remains motionless:

$$({}^0\mathbf{A}_\pi)_i = ({}^0\mathbf{A}_S)_i = [{}^0\mathbf{s}_\pi \;\; {}^0\mathbf{n}_\pi \;\; {}^0\mathbf{a}_\pi]_i \quad (9)$$

where ${}^0\mathbf{A}_\pi$ represents the rotation matrix between frames R_π and R_0 (Fig. 3). The elementary movement of the robot is done on the plane defined by $(\Omega, \bar{\mathbf{a}})$.

So, the problem is to determine the elementary variation of the state sub-vector $\mathbf{Y} = [x, y, z, \psi]^t$. The new

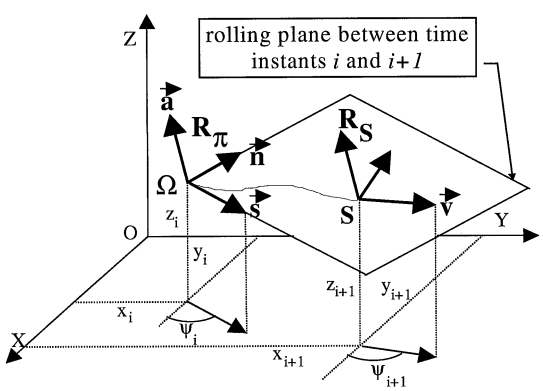

Fig. 3. Elementary motion in the plane defined by the last estimated position and the inclinometers.

values of dc and dv are directly given by the inclinometer measurements (α, β).

$$\text{in } R_0 \begin{cases} x_{i+1} = x_i + \delta x(\mathbf{Y}_i, \mathbf{U}_i, \alpha_i, \beta_i) \\ y_{i+1} = y_i + \delta y(\mathbf{Y}_i, \mathbf{U}_i, \alpha_i, \beta_i) \\ z_{i+1} = z_i + \delta z(\mathbf{Y}_i, \mathbf{U}_i, \alpha_i, \beta_i) \\ \psi_{i+1} = \psi_i + \delta\psi(\mathbf{Y}_i, \mathbf{U}_i, \alpha_i, \beta_i) \end{cases} \tag{10}$$

In other words, the aim is to compute now the elementary rotation and translation in R_0

$$d\vec{\mathbf{R}}_i = {}^0[0 \quad 0 \quad \delta\psi_i]^T \tag{11}$$

$$d\vec{\mathbf{T}}_i = {}^0[\delta x_i \quad \delta y_i \quad \delta y_i]^T. \tag{12}$$

In order to simplify the equations, the subscripts 'i' will be omitted in the equations that follow.

4.1.2. Elementary translation (δx, δy, δz) in R_0

Knowing $\mathbf{U}$, $d\vec{\mathbf{T}}$ can be expressed in R_π. The robot is supposed to perform first a translation of length Δ and then a rotation of angle ω. This evolution model is a simplification of the classical one presented in (Bonnifait and Garcia, 1996)

$${}^\pi d\mathbf{T} = [\Delta \quad 0 \quad 0]^T. \tag{13}$$

In R_0, the coordinates of this vector are

$${}^0 d\mathbf{T} = [\delta x \quad \delta y \quad \delta z]^T = {}^0\mathrm{A}_\pi \, {}^\pi d\mathbf{T} \tag{14}$$

After computation

$$\delta x = \Delta \cos(\alpha)\cos(\psi) \tag{15}$$

$$\delta y = \Delta \cos(\alpha)\sin(\psi) \tag{16}$$

$$\delta z = \Delta \sin(\alpha). \tag{17}$$

4.1.3. Elementary rotation $\delta\psi$ in R_0

The rotation vector $d\vec{\mathbf{R}}$ in the frame R_π is obtained from the elementary rotation ω measured in the rolling plane owing to the encoders

$${}^\pi\mathbf{R} = [0 \quad 0 \quad \omega]^t. \tag{18}$$

Hence, in R_0,

$${}^0 d\mathbf{R} = {}^0\mathbf{A}_\pi \, {}^\pi d\mathbf{R}. \tag{19}$$

The third component of ${}^0 d\vec{\mathbf{R}}$ is the projection of $d\vec{\mathbf{R}}$ on the z_0 axis of R_0 and is the variation on ψ: After computation

$$\delta\psi = \omega\sqrt{\cos(\alpha)^2 - \sin(\beta)^2} \tag{20}$$

4.2. Prediction phase with odometry

The plant model for the state is adapted from equations (10), (15)–(17) and (20), but the evolution model for dc and dv is a constant. The evolution is allowed thanks to the model noise $[\alpha_{dc}, \alpha_{dv}]^T$. If the variance of this noise becomes small, the overall effect of the EKF for dc and dv is similar to a 'low-pass' filter applied to their measurements. This can be of great use, in real situations, to filter the vibrations induced by the engine.

The plant model is then

$$\begin{cases} x_{i+1} = x_i + \Delta_i \cos(dc_i)\cos(\psi_i) + \alpha_x \\ y_{i+1} = y_i + \Delta_i \cos(dc_i)\sin(\psi_i) + \alpha_y \\ z_{i+1} = z_i + \Delta_i \sin(dc_i) + \alpha_z \\ \psi_{i+1} = \psi_i + \omega_i\sqrt{\cos(dc_i)^2 - \sin(dv_i)^2} + \alpha_\psi \\ dc_{i+1} = dc_i + \alpha_{dc} \\ dv_{i+1} = dv_i + \alpha_{dv} \end{cases} \tag{21}$$

$$\Leftrightarrow \{\mathbf{X}_{i+1} = \mathbf{F}(\mathbf{X}_i, \mathbf{U}_i) + \alpha_{\mathbf{x}}. \tag{22}$$

Since the noise on the encoders (the variance of which is denoted $\mathbf{Q}_U$) is clearly independent of the state, the predicted variance of $\mathbf{X}$ can be computed by a classical Taylor expansion (Bonnifait and Garcia, 1996)

$$\mathbf{P}_{i+1/i} = \left(\frac{\partial \mathbf{F}}{\partial \mathbf{X}}\right)\mathbf{P}_{i/i}\left(\frac{\partial \mathbf{F}}{\partial \mathbf{X}}\right)^T_{\hat{\mathbf{X}}_{i/i}} + \left(\frac{\partial \mathbf{F}}{\partial \mathbf{U}}\right)\mathbf{Q}_U\left(\frac{\partial \mathbf{F}}{\partial \mathbf{U}}\right)^T_{\mathbf{U}_{i+1}} + \mathbf{Q}_\alpha \tag{23}$$

4.3. Estimation phase with the inclinometers

In this section, the classical Kalman filtering formulation, presented by Chen et al. (1994), is applied, with the observation equation given by:

$$\begin{pmatrix} \alpha_i \\ \beta_i \end{pmatrix} = \begin{bmatrix} 0 & 0 & 0 & 0 & 1 & 0 \\ 0 & 0 & 0 & 0 & 0 & 1 \end{bmatrix}\mathbf{X}_i = \mathbf{C}\mathbf{X}_i \tag{24}$$

Knowing the variance $\mathbf{Q}_{\text{inc}}$ of the inclinometers, the Kalman gain is computed

$$\mathbf{K} = \mathbf{P}_{i+1/i}\mathbf{C}^T(\mathbf{C}\mathbf{P}_{i+1/i}\mathbf{C}^T + \mathbf{Q}_{\text{inc}})^{-1}. \tag{25}$$

The updated estimate and its associated estimated covariance matrix are then given by:

$$\hat{\mathbf{X}}_{l+1/l+1} = \hat{X}_{l+1/l} + \mathbf{K}\left(\begin{pmatrix} \alpha_{i+1} \\ \beta_{i+1} \end{pmatrix} - \mathbf{C}\hat{\mathbf{X}}_{i+1/i}\right) \tag{26}$$

$$\mathbf{P}_{i+1/i+1} = (\mathbf{I} - \mathbf{K}\mathbf{C})\,\mathbf{P}_{i+1/i} \tag{27}$$

4.4. Correction phase with the exteroceptive sensor

At time j, when an asynchronous optical measure occurs, the predicted sub-vector $[x, y, z, \psi]^t$ is corrected. Thanks to this step, estimation errors on these parameters do not drift. In order to express the relations between the measurement angles (λ, σ) and the state $\mathbf{X}$, the position of the beacon in the frame R_S of the exteroceptive sensor has to be determined.

In R_0, the known homogeneous position of the beacon is defined by:

$${}^0\mathbf{P}_B = [{}^0x_B \;\; {}^0y_B \;\; {}^0z_B \;\; 1]^T \tag{28}$$

Let ${}^0\mathbf{T}_S$ denote the homogeneous transformation matrix of the sensor frame relative to R_0.

$$ {}^0\mathbf{T}_s = \begin{bmatrix} & {}^0\mathbf{A}_s & & x \\ & & & y \\ & & & z \\ 0 & 0 & 0 & 1 \end{bmatrix} \Leftrightarrow {}^0\mathbf{T}_s = \begin{bmatrix} {}^0\mathbf{A}_s & {}^0\mathbf{P}_s \\ 0 \quad 0 \quad 0 & 1 \end{bmatrix} \tag{29} $$

In R_S, Eq. (28) becomes

$$ {}^s\mathbf{P}_B = {}^s\mathbf{T}_0\,{}^0\mathbf{P}_B = \begin{bmatrix} {}^0\mathbf{A}_s^t & -{}^0\mathbf{A}_s^t\,{}^0\mathbf{P}_s \\ \mathbf{0} & \mathbf{1} \end{bmatrix} {}^0\mathbf{P}_B. \tag{30} $$

After calculation, using Eqs. (1), (29) and (30)

$$ s_{x_B} = -\cos(dc)\,[\cos(\psi)(x - {}^0x_B) + \sin(\psi)(y - {}^0y_B)] - \sin(dc)(z - {}^0z_B) \tag{31} $$

$$ s_{y_B} = \left[\frac{\sin(\psi)\chi}{\cos(dc)} - \tan(dc)\sin(dv)\cos(\psi)\right](x - {}^0x_B) - \left[\tan(dc)\sin(dv)\sin(\psi) + \frac{\cos(\psi)\chi}{\cos(\mathrm{dc})}\right](y - {}^0y_B) + \sin(dv)(z - {}^0z_B) \tag{32} $$

$$ s_{z_B} = \left[\frac{\sin(\psi)\sin(dv)}{\cos(dc)} + \cos(\psi)\tan(dc)\,\chi\right](x - {}^0x_B) + \left[\frac{-\cos(\psi)\sin(dv)}{\cos(dc)} + \sin(\psi)\tan(dc)\,\chi\,(y - {}^0y_B) - \chi(z - {}^0z_B). \right. \tag{33} $$

Finally, the two observation equations (see Fig. 1) are given by

$$ \begin{cases} \lambda_j = \mathrm{a}\tan 2({}^sy_b, {}^sx_b) \\ \sigma_j = \arctan\left(\dfrac{{}^sz_b}{\sqrt{{}^sx_b^2 + {}^sy_b^2}}\right) \end{cases} \Leftrightarrow \begin{pmatrix} \lambda_j \\ \sigma_j \end{pmatrix} = \mathbf{G}_b(\mathbf{X}_j) \tag{34} $$

The subscript b of function $\mathbf{G}_b$ means that these equations depend on the landmark that has been detected. Thus, the observation equation is, in this phase, non-stationary.

The Kalman filter formulation is identical to the one shown in Section 4.3. Instead of (α, β), (λ, σ) are used; $\mathbf{C}$ is replaced by the Jacobian matrix $(\partial\mathbf{G}_b/\partial\mathbf{X})$ because the observation equation is not linear. Moreover, $\mathbf{Q}_{\mathrm{inc}}$ is replaced by $\mathbf{Q}_s$ which represents the goniometric errors.

4.5. Overview of the algorithm

The dynamic localization method is described by the following algorithm:

Begin
  Static localization, filter initialization
  Do
    U = read odometric data
    (**X**, **P**) = prediction phase (X, P, U)
    I = read inclinometers data
    (**X**, **P**) = estimation phase (X, P, I)
    if (external measure Λ) do
      (**X**, P) = correction phase (X, P, Λ)
    End if.
  End loop at the frequency of 20 Hz
End.

5. Simulation results

Simulations have been performed with SimuCIRC (Bétaille and Peyret, 1997), a specialized computer integrated road construction software package, based on Matlab and Simulink. Gaussian random noises have been added to the measurements. In particular, the variance of the errors of the inclinometers has been multiplied by two, in order to compensate for the effects of the vibrations and accelerations of the machine. Noise variances for the goniometric sensor and for the encoders are those of the real sensors, already used in Bonnifait and Garcia (1996) and Le Corre and Garcia (1992).

5.1. Real trajectory

The real trajectory corresponds to the curves of Figs. 4–7, with a constant projected speed of 0.1 m/s, in (O, x_0, y_0). The projected path of Fig. 4 is made up of a straight line, a semicircle and a straight line (see beacon location). Figs. 5, 7 and 8 show the altitude, dc and dv as functions of the curvilinear abscissa in (O, x_0, y_0). During the first line, the elevation follows a linear variation, whereas after the semicircle, the variation is parabolic. Finally, the cross-section is horizontal, except in the semicircle, as plotted in Fig. 7.

The principle of the simulation is to have a modeled robot which follows this 3D path. While it is moving,

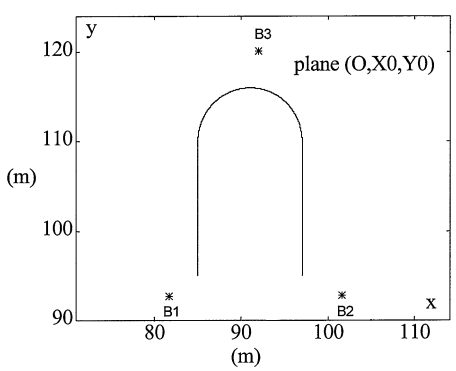

Fig. 4. Projection of the real path.

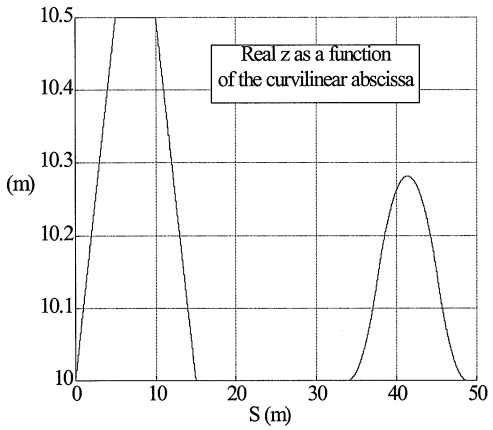

Fig. 5. Altitude along the real path.

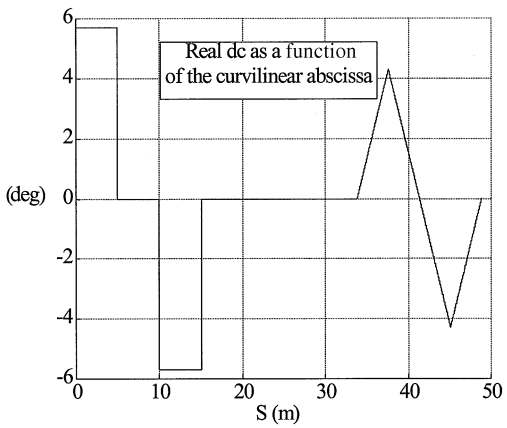

Fig. 6. Gradient along the real path.

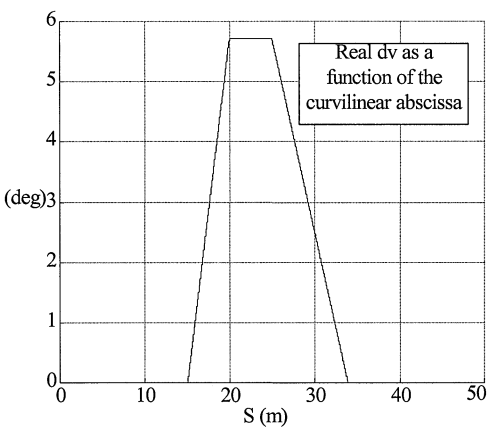

Fig. 7. Cross-fall along the real path.

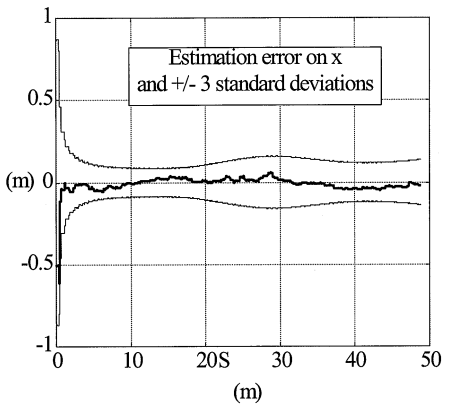

Fig. 8. x estimation.

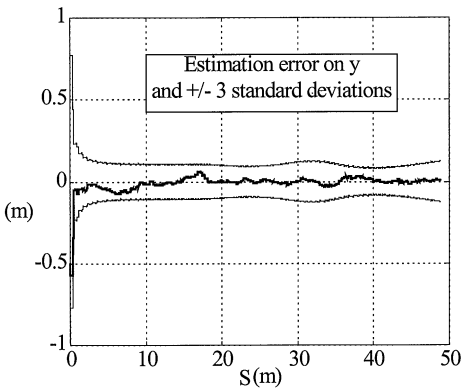

Fig. 9. y estimation.

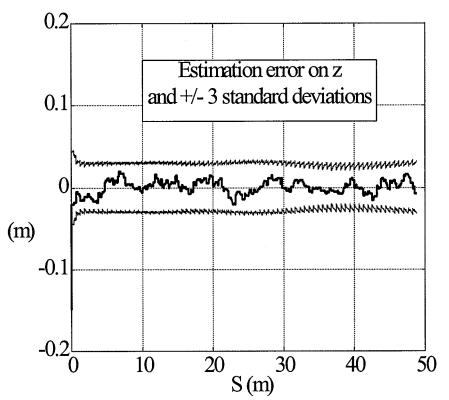

Fig. 10. Altitude estimation.

inclinometer and odometric measurements are calculated. The rotation of the camera is also modeled; therefore, the asynchronicity of the azimuth and elevation angles is taken into account.

5.2. State estimation analysis

Even if the EKF is initialized with significantly large errors (50 cm error on xy, 15 cm on z, 2 degrees on Ψ and 1 degree on dc and dv), the transient phase is short, as shown in Figs. 8–11.

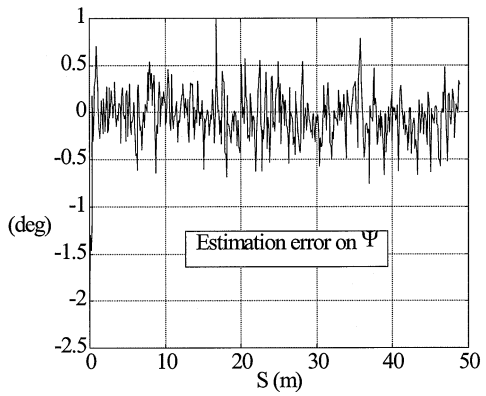

Fig. 11. Direction estimation.

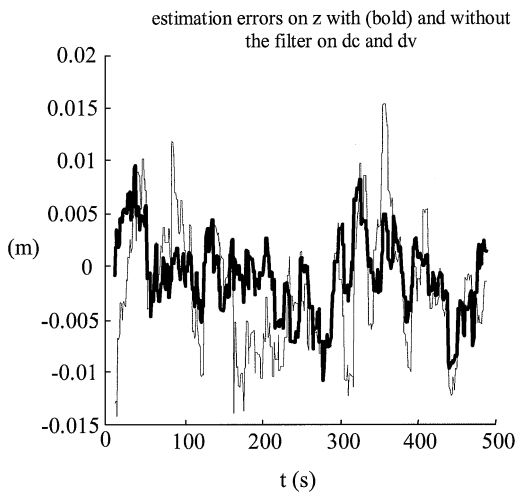

Fig. 12. Altitude estimation.

The global estimation process has a good behavior, since the errors have zero means. Moreover, they are far lower than three estimated standard deviations, as exemplified by Figs. 8–10: this condition is necessary for a good EKF process.

The 2D behavior, i.e. the estimation of the sub-vector $[x, y, \psi]^T$ (Figs. 8, 9 and 11), is close to the one encountered with real data (see Bonnifait and Garcia, 1996). The distance error is of the order of a few centimeters (< 0.05 m), and the heading error standard deviation is equal to 0.4°.

In Fig. 10, the zero mean elevation error remains bounded by 1 cm. Its shape does not depend on either the longitudinal-section or the cross-section. This proves that the 3D odometric evolution is good. The filtering of the inclinometers is of particular importance since, in addition to reducing errors on *dc* and *dv*, it also significantly improves the elevation estimation (Fig. 12). Indeed, oscillations and peaks are filtered. This is an interesting aspect of the filter: by applying a 'low-pass' filter on *dc* and *dv*, the *z* estimation is improved.

6. Real experiments

Real experiments have been carried out with an outdoor mobile robot. The computations of the location data are done at 20 Hz with a 486 DX 33 PC-type computer. On a lawn, a 0.5 m × 8 m bridge has been put parallel to the x axis of the reference frame. Fig. 13 describes a typical experiment. First, when the robot is motionless and when three different beacons have been detected, a static localization is computed. Afterwards, the robot starts to move at a constant speed equal to 0.06 m/s until the end of the bridge.

This section is devoted to the results of the altitude estimation, since this parameter is the most crucial one for the CIRC application. The errors on the x and y parameters are of the same order as the ones reported in Bonnifait and Garcia (1996), i.e. of the order of 5 cm.

In Fig. 14, the results of two experiments are reported. These tests correspond to the same trajectory, and the displacement is done from $x = 96$ to $x = 84$. The curves of Fig. 14 show that the repeatability of the altitude estimation is very good: the distance between the curves is bounded by one centimeter, except at the beginning of the slope. This discrepancy can be explained by the fact that the ground was extremely muddy at this spot, and altered in successive tests, due to the weight of the robot.

The precision of the altitude estimated by the positioning system cannot be precisely determined with this experimental set-up: a benchmark system has to be used. Nevertheless, for a static position, the altitude of the EKF has been compared with that of a differential Global Position System (GPS) running a real-time kinematic algorithm. The precision of this kind of GPS

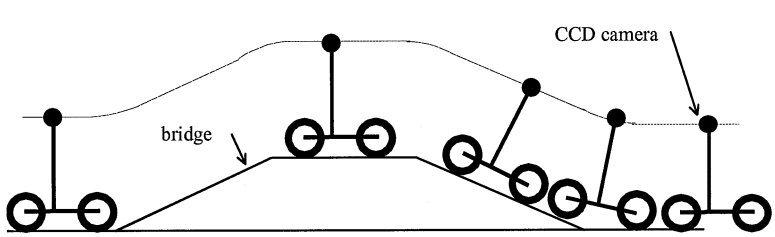

Fig. 13. The mobile robot moving on the bridge.

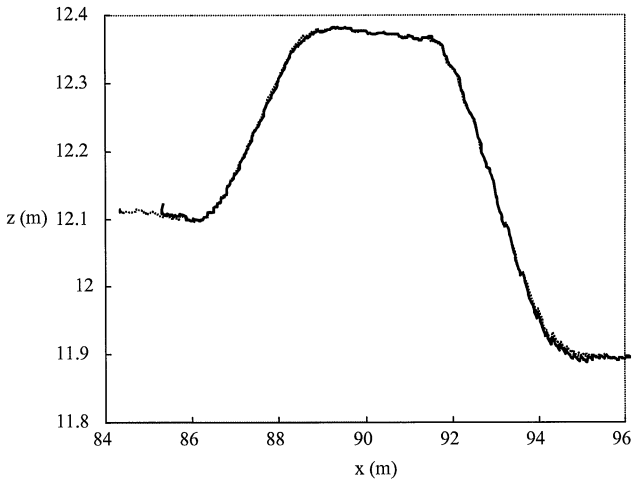

Fig. 14. Estimated altitude as a function of the estimated abscissa.

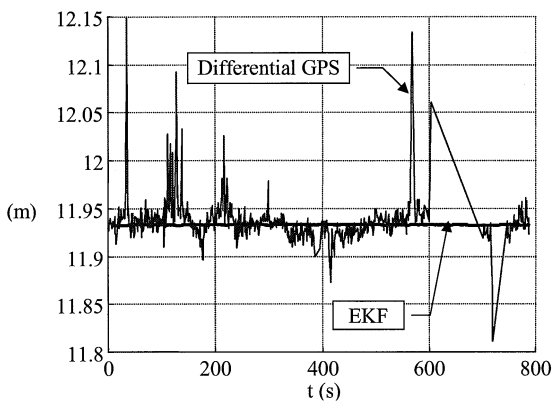

Fig. 15. Altitude computed by the EKF compared to a differential GPS on a static position.

receiver is of the order of centimeters on average, and typically better than two centimeters if the averaging period is 'sufficiently' long. For the 13-min experiment reported in Fig. 15, the averaged altitude of the GPS is equal to 11.94 m. The distance between this value and the altitude estimated by the EKF is less than 1 mm. This of course does not prove that when moving the precision of the EKF is still of the order of 1 cm; it only ascertains that the optical system is well calibrated.

7. Conclusions and future work

In this paper, a localization system based on 3D-odometry and external goniometry has been presented. This system is intended for slow-dynamics outdoor vehicles, requiring a high precision in their altitude.

The 3D-odometric equations use measurements from two inclinometers and two encoders. The estimated state exhibits the tilt sensor measurements, thanks to an unusual attitude representation in robotics, based on the orthogonal cross-fall and gradient angles. The updating of the dead-reckoning location is performed by a six-state EKF which allows each goniometric measurement to be taken into account individually and asynchronously.

Furthermore, simulations indicate that the precision on the altitude can be better than 1 cm, if a low-pass filter is applied to the inclinometer data. Real experiments with this algorithm have been performed with a mobile robot moving on an outdoor test-track. The tuning of the EKF running on real data has been made easier thanks to the simulations, and the same behavior of the filter has been noted. These first tests indicate that the optical system is well calibrated, and they prove that unmodelled low accelerations do not degrade the inclinometer measurements. When the vehicle is moving, the altitude accuracy cannot be determined precisely, but is clearly of the order of centimeters. Moreover, the repeatability of the altitude estimation is better than 1 cm.

Future work will involve benchmarking this multi-sensor localization system on the special test track, 'SESSYL', of the Laboratoire Central des Ponts et Chaussées of France. SESSYL is a robotized head with three degrees of freedom, mounted on a carriage that moves along a calibrated rail.

References

Barshan, B., & Durrant-Whyte H.F. (1995). Inertial navigation systems for mobile robots. *IEEE Trans. Rob. Auto.*, *11*(3), 328–342.

Bétaille, D., & Peyret, F. (1997). A simulator for road construction equipment. *Int. Symp. Auto. Rob.* Construction, Pittsburgh (pp. 451–458).

Bonnifait, Ph., & Garcia, G. (1996). A multisensor localization algorithm and its real-time experimental validation. *IEEE Int. Conf. on Rob. and Auto.* Minneapolis (pp. 1395–1400).

Chen, J.-H., Lee, S.C., & Debra, D.B. (1994). Gyroscope free strapdown inertial measurement unit by six linear accelerometers. *J. Guidance Control Dyn.*, *17*(2), 286–290.

Fuke, Y., & Krotkov, E. (1996). Dead reckoning for a lunar rover on uneven terrain. *IEEE Int. Conf. on Rob. & Auto.*, Minneapolis (pp. 441–416).

Kim, K.R., Lee, J.C., Kim, J.H., (1996). Dead-reckoning for a two-wheeled mobile robot on curved surfaces. *IEEE Int. Conf. on Rob. and Auto*, Minneapolis (pp. 1732–1737).

Horn, J., & Schmidt, G. (1995). Continuous localization of a mobile robot based on 3D-laser-range-data, predicted sensor images, and dead-reckoning. *Rob. Autonomous Systems* (2-3), 99–118.

Le Corre, J.-F., & Garcia, G. (1992). Real-time determination of the location and speed of mobile robots running on non-planar surfaces. *IEEE Int. Conf. on Rob. and Auto*, Nice (pp. 2594–2599).

Rintanen, K., Kauppi, I., Koskinen, K., & Koskinen, A. (1994). Inertial navigation for mobile robots by redundant low-cost gyrometers. *Int. Conf. on Machine Automation*, Tampere (pp. 225–241).

Tsumura, T., Okubo, H., Komatsu, N. (1993). A 3D position and attitude measurement system using laser scanners and corner cubes. *IEEE/RSJ Int. Symp. on Int. Rob. and Sys*, Yokohama (pp. 604–611).

Vaganay, J., Aldon, M.J., & Fournier, A. (1993). Mobile robot attitude estimation by fusion of inertial data. *IEEE Int. Conf. on Rob. Atlanta. and Auto* (pp. 277–282).